Cardiac myocyte follistatin-like 1 functions to attenuate hypertrophy following pressure overload

Masayuki Shimano[a], Noriyuki Ouchi[a], Kazuto Nakamura[a], Bram van Wijk[b], Koji Ohashi[a], Yasuhide Asaumi[a], Akiko Higuchi[a], David R. Pimentel[a], Flora Sam[a], Toyoaki Murohara[c], Maurice J. B. van den Hoff[b], and Kenneth Walsh[a,1]

[a]Whitaker Cardiovascular Institute, Boston University, Boston, MA 02118; [b]Department of Anatomy, Embryology, and Physiology, Heart Failure Research Center, Academic Medical Center, 1105 AZ, Amsterdam, The Netherlands; and [c]Department of Cardiology, Nagoya University Graduate School of Medicine, Nagoya, Aichi 466-8550, Japan

Edited by Eric N. Olson, University of Texas Southwestern, Dallas, TX, and approved September 13, 2011 (received for review May 31, 2011)

Factors secreted by the heart, referred to as "cardiokines," have diverse actions in the maintenance of cardiac homeostasis and remodeling. Follistatin-like 1 (Fstl1) is a secreted glycoprotein expressed in the adult heart and is induced in response to injurious conditions that promote myocardial hypertrophy and heart failure. The aim of this study was to investigate the role of cardiac Fstl1 in the remodeling response to pressure overload. Cardiac myocyte-specific Fstl1-KO mice were constructed and subjected to pressure overload induced by transverse aortic constriction (TAC). Although Fstl1-KO mice displayed no detectable baseline phenotype, TAC led to enhanced cardiac hypertrophic growth and a pronounced loss in ventricular performance by 4 wk compared with control mice. Conversely, mice that acutely or chronically overexpressed Fstl1 were resistant to pressure overload-induced hypertrophy and cardiac failure. Fstl1-deficient mice displayed a reduction in TAC-induced AMP-activated protein kinase (AMPK) activation in heart, whereas Fstl1 overexpression led to increased myocardial AMPK activation under these conditions. In cultured neonatal cardiomyocytes, administration of Fstl1 promoted AMPK activation and antagonized phenylephrine-induced hypertrophy. Inhibition of AMPK attenuated the antihypertrophic effect of Fstl1 treatment. These results document that cardiac Fstl1 functions as an autocrine/paracrine regulatory factor that antagonizes myocyte hypertrophic growth and the loss of ventricular performance in response to pressure overload, possibly through a mechanism involving the activation of the AMPK signaling axis.

TSC-36 | angiogenesis

Proper communication between different cell types in the heart is required to maintain cardiac homeostasis and mount appropriate responses to stress. Pressure overload-induced cardiac hypertrophy is initially an adaptive response, but sustained hypertrophy of the myocardium can lead to left ventricular (LV) systolic dysfunction (1, 2). Therefore, a better understanding of the factors that regulate cardiac hypertrophy could lead to the development of new therapies for the treatment of heart failure (3). To identify therapeutic targets in the heart, a number of recent studies have sought to isolate and characterize secreted proteins that affect cardiac remodeling via endocrine, paracrine, or autocrine mechanisms (4–10). One such protein produced by the heart is follistatin-like 1 (Fstl1), a 308-amino acid, extracellular glycoprotein (11, 12). To understand the role of Fstl1 in heart, we sought to identify the cell types that produce and respond to this factor and to characterize the functional response of the heart to stress when Fstl1 levels are manipulated genetically.

Fstl1, also referred to as "TSC-36," was identified originally in a murine osteoblastic cell line as a TGF-β–inducible gene (13, 14). Although Fstl1 is categorized as a follistatin-like protein, it has relatively limited homology with other follistatin family proteins that classically act as binding partners of the TGF-β family proteins. In contrast to follistatin and Fstl3, Fstl1 can function as a ligand for a cell-surface receptor, and it does not appear to act as a high-affinity extracellular regulator of activin A-stimulated Sma- and Mad-related protein (Smad) phosphorylation in cardiovascular cells (7, 15, 16). Previous studies have implicated a role for Fstl1 in inflammatory responses and in the control of tumor cell growth in vitro (17–20).

The involvement of Fstl1 in cardiovascular tissue regulation was indicated when the up-regulation of its transcript was identified in the hearts of cardiac-specific Akt transgenic mice (9, 21). Subsequently, it was shown that Fstl1 expression in the heart is induced by ischemic insults and that the systemic administration of an adenoviral vector expressing Fstl1 protects the heart from ischemia/reperfusion injury (11). Previous studies have shown that the *Fstl1* transcript is expressed in explanted human failing heart and that circulating Fstl1 level is increased in patients with acute coronary syndrome or heart failure (12, 22, 23). Therefore, Fstl1 appears to be a clinically relevant secreted protein that participates in the pathophysiological responses to cardiovascular stress.

Although it has been reported that *Fstl1* transcript expression is up-regulated in the myocardium in response to experimental pressure overload (11), nothing is known about the role of Fstl1 in the control of cardiac hypertrophy. To address this question, we constructed mouse lines that are deficient for Fstl1 expression in cardiac myocytes and that transgenically overexpress Fstl1. We used these models to investigate the role of Fstl1 in pressure-overload hypertrophy and heart failure.

Results

Cardiac Myocyte-Specific Fstl1-KO Mice. To evaluate the role of Fstl1 in the heart, cardiomyocyte-selective KO mice were constructed by breeding $Fstl1^{flox/flox}$ mice with αMHC-$Cre^{+/-}$ transgenic mice to ablate the second exon of the *Fstl1* gene in cardiac myocytes. KO mice (αMHC-$Cre^{+/-}$ × $Fstl1^{flox/flox}$) and WT FVB mice (αMHC-$Cre^{+/-}$ × $Fstl1^{+/+}$) initially were examined for Fstl1 expression at baseline and in response to pressure overload caused by transverse aortic constriction (TAC). Quantitative PCR (qPCR) and Western blot analysis of whole-heart extracts from sham surgery demonstrated 42% and 46% reductions of Fstl1 transcript and protein levels, respectively, in KO mice relative to WT mice at baseline (Fig. 1*A* and *B*). In WT mice, TAC led to 9.5- and 2.1-fold increases in the levels of Fstl1 transcript and protein, respectively, but TAC-induced levels of Fstl1 transcript and protein were markedly reduced in the KO strain. Adult cardiac myocytes were prepared from KO and WT mice and subjected to Western blot analysis (Fig. 1*C*). Fstl1 protein levels were reduced by >95% in myocytes prepared from KO mice,

Author contributions: M.S. and K.W. designed research; M.S., N.O., K.N., K.O., Y.A., and A.H. performed research; B.v.W., K.O., Y.A., A.H., D.R.P., F.S., T.M., and M.J.B.v.d.H. contributed new reagents/analytic tools; M.S., N.O., K.N., F.S., T.M., and M.J.B.v.d.H. analyzed data; and M.S., K.N., and K.W. wrote the paper.

The authors declare no conflict of interest.

This article is a PNAS Direct Submission.

[1]To whom correspondence should be addressed. E-mail: kxwalsh@bu.edu.

See Author Summary on page 17581.

This article contains supporting information online at www.pnas.org/lookup/suppl/doi:10.1073/pnas.1108559108/-/DCSupplemental.

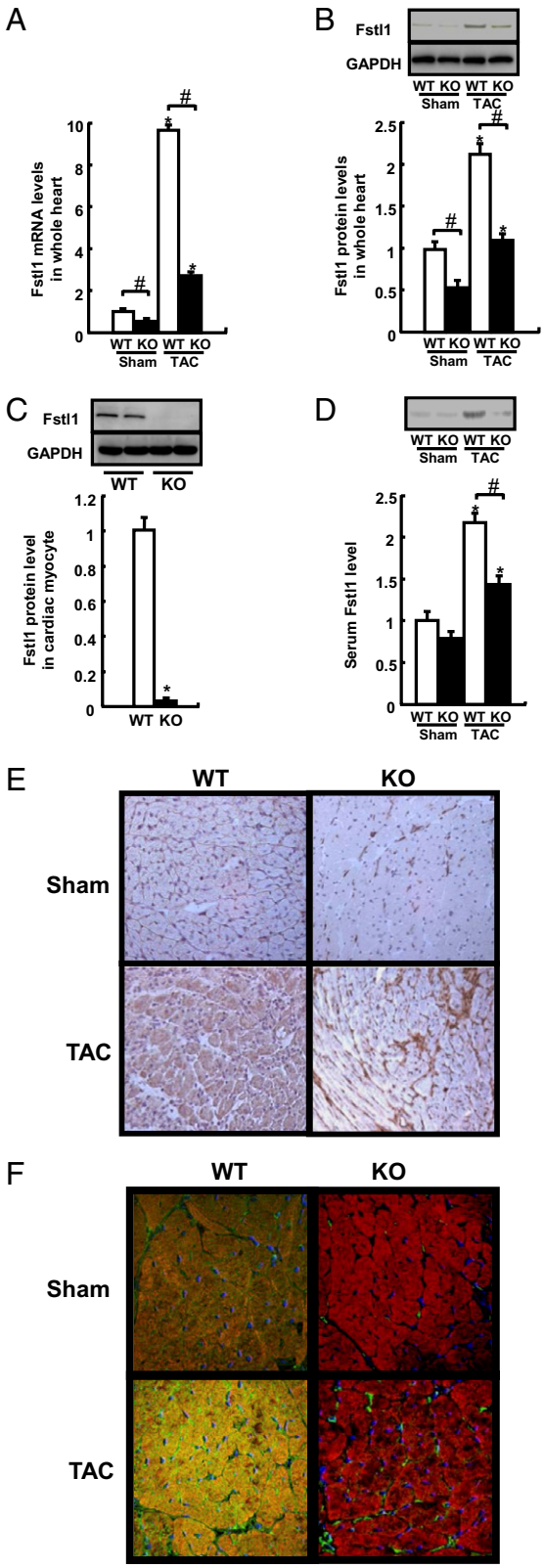

Fig. 1. Expression of Fstl1 in heart. (*A* and *B*) Changes in Fstl1 transcript (*A*) and protein (*B*) in the hearts of WT and cardiac myocyte-specific Fstl1-KO mice 1 wk after TAC or sham surgery. Representative blots of Fstl1 and GAPDH are shown in *B*. (*C*) Fstl1 protein levels in isolated cardiac myocytes. Western blot analysis was performed to evaluate Fstl1 protein expression in cardiac myocytes isolated from WT or KO mice. (*D*) Fstl1 protein levels in serum from WT and KO mice 1 wk after TAC or sham surgery. A representative blot for Fstl1 is shown. (*E*) Immunochemical staining of Fstl1 in cardiac sections from WT or KO mice 4 wk after sham or TAC operation. Myocardial tissues from WT or KO mice were fixed and incubated with Fstl1 antibody, followed by incubation with biotin-conjugated secondary antibody and HRP-avidin. (*F*) Immunofluorescence of Fstl1 (green; Alexa Fluor 488) and α-actinin (red; Alexa Fluor 594) in cardiac sections from WT or KO mice 4 wk after sham or TAC operation. Blue is DAPI. $^{*}P < 0.05$ versus corresponding sham-treated mice; $^{\#}P < 0.05$ versus corresponding WT mice.

suggesting that the residual expression of Fstl1 in KO mouse hearts is likely the result of Fstl1 expression in nonmyocytes such as fibroblasts or vascular cells.

Circulating levels of Fstl1 protein also were assessed under these experimental conditions (Fig. 1*D*). TAC led to a 2.2-fold increase in serum Fstl1 levels in WT mice. This induction was reduced markedly in the KO mice, indicating that cardiac myocytes are the major source of secreted Fstl1 in mice that are subjected to TAC surgery.

Previously, Lara-Pezzi, et al. (12) reported that Fstl1 is expressed in myocytes and vascular cells in explanted human heart specimens. To determine the cellular distribution of Fstl1 protein in our model, heart sections from sham or TAC conditions were immunostained with an antibody directed against Fstl1 (Fig. 1*E*). Low levels of Fstl1 protein could be detected in myocytes of sham-treated WT mice, but a higher signal could be detected in the less frequently observed interstitial cells. TAC led to the accumulation of Fstl1 within the myocytes of WT mice, but Fstl1 signal within myocytes was not observed in Fstl1-KO hearts at baseline or following TAC.

To examine the cell type-specific expression of Fstl1 in greater detail, tissue sections of WT and Fstl1 hearts were immunostained for Fstl1 and the myocyte marker α-actinin and analyzed by confocal microscopy (Fig. 1*F*). Dual-image analysis of Fstl1 (green) and α-actinin (red) showed a colocalization signal (yellow) in WT mice, and the intensity of colocalized signal was increased markedly by TAC surgery. No colocalization was detected in Fstl1-KO heart sections, but Fstl1 signal could be observed in less common nonmyocyte cells within these sections. Of note, the frequency of these Fstl1-positive, α-actinin–negative cells increased in response to TAC in both WT and KO mice. This increase in nonmyocyte Fstl1 signal is consistent with the small but significant increase in Fstl1 transcript and protein observed in whole hearts of KO mice subjected to TAC (Fig. 1 *A* and *B*).

Collectively, these data show that the induction of Fstl1 expression by TAC, at the levels of tissue transcript, tissue protein, or serum protein, is largely abolished in the cardiac myocyte-specific Fstl1-KO mice. Although injury-induced levels of Fstl1 are derived predominantly from cardiac myocytes in this model, cardiac Fstl1 is expressed appreciably by both cardiac myocytes and nonmonocytes at baseline.

Fstl1-Deficiency in Cardiac Myocytes Exacerbates Hypertrophy and Dysfunction Following Pressure Overload. Fstl1-KO mice did not exhibit a detectable baseline phenotype. Compared with control mice (αMHC-Cre$^{+/-}$ × Fstl1$^{+/+}$), these animals had a normal heart weight to body weight ratio (HW/BW), a normal lung weight to body weight ratio (LW/BW), and normal echocardiographic parameters such as ventricular thickness, ventricular dimension, and contractility; hearts appeared normal upon histological examination (Figs. 2 *A–F* and 3 *A–C*). In contrast, Fstl1-KO mice demonstrated a significantly greater cardiac growth response following 4 wk of TAC stimulation (Fig. 2*A*). After 4 wk of TAC, WT FVB mice displayed a 26% increase in HW/BW ratio, whereas Fstl1-KO mice displayed a 39% increase (Fig. 2*A*). TAC led to an increase in LW/BW ratio in both experimental groups, but the Fstl1-KO mice displayed a greater degree of pulmonary congestion (Fig. 2*B*). No differences in these parameters were detected either at baseline or following

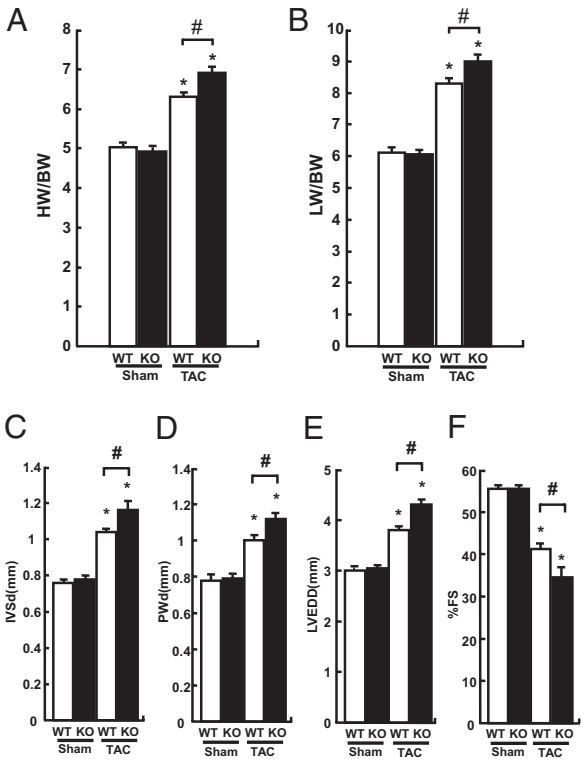

Fig. 2. Loss of Fstl1 expression in myocytes promotes pressure overload-induced cardiac hypertrophy and heart failure. (*A* and *B*) HW/BW (*A*) and LW/BW (*B*) ratios in WT and cardiac myocyte-specific Fstl1-KO mice 4 wk after TAC or sham surgery. (*C–F*) Echocardiographic parameters in different experimental groups of mice. Shown are measurements of IVSd (*C*), PWd (*D*), LVEDD (*E*), and %FS (*F*) for WT and KO mice 4 wk after TAC or sham surgery. For sham-treated mice, $n = 8$ WT mice and 8 KO mice. For TAC-treated mice, $n = 16$ WT mice and 14 KO mice. $^{*}P < 0.05$ versus corresponding sham; $^{\#}P < 0.05$ versus corresponding WT mice.

TAC in WT mice that were either positive or negative for the Cre transgene.

Consistent with the increased HW/BW ratio in Fstl1-KO mice at 4 wk after TAC, assessment by echocardiography showed, as expected, an increase in septal and LV wall thickness compared with controls (Fig. 2 *C* and *D*). Echocardiographic assessment of ventricular performance showed increased LV dimension and reduced fractional shortening, indicative of decompensated hypertrophy (Fig. 2 *E* and *F*).

Cardiomyocyte cell size and LV interstitial fibrosis were evaluated in histological sections. Compared with WT mice, FStl1-KO mice displayed greater increases in myocyte hypertrophy and fibrosis 4 wk post-TAC (Fig. 3 *A–C*). In addition, the ablation of Fstl1 in cardiac myocytes elevated the TAC-induced increases in brain natriuretic peptide (BNP) and atrial natriuretic factor (ANF) gene expression (Fig. 3 *D* and *E*). Consistent with the enhanced pathological remodeling of the Fstl1-deficient heart, a reduction of myocardial capillary density could be detected under these conditions (Fig. S1).

Accumulating evidence indicates that the AMP-activated protein kinase (AMPK) signaling axis functions to suppress cardiac hypertrophy (24, 25). To examine the possible participation of AMPK in this model of pressure overload-induced heart failure, the activating phosphorylation of cardiac AMPK at Thr172 of the α2 subunit was assessed by Western blot analysis. The myocardial expression of total AMPK protein did not differ between KO and WT mice or in response to TAC surgery. The phosphorylation of AMPK at Thr172 of the α subunit was increased in response to TAC, but this response was reduced significantly in the Fstl1-KO mouse hearts that displayed a greater hypertrophic response (Fig. 3*F*). There were no differences in the low level of AMPK phosphorylation in sham-operated hearts in Fstl1-KO and WT mice. Fstl1-deficient mice displayed a reduction in cardiac endothelial nitric-oxide synthase (eNOS) phosphorylation at Ser1179, a downstream target of AMPK, under conditions of TAC (Fig. S2). In contrast, no changes were observed in the phosphorylation of cardiac SMAD-2.

Mice Overexpressing Fstl1 Are Protected from Pressure-Overload Cardiac Hypertrophy and Remodeling. Because the loss of Fstl1 led to an exaggerated hypertrophic response to TAC, it was of interest to examine mice that overexpress this factor. To investigate the effects of Fstl1 gain of function, transgenic (Fstl1-TG) mice were constructed expressing full-length murine Fstl1 downstream of the creatine kinase M promoter that is expressed in both cardiac and skeletal muscle. Fstl1-TG mice displayed increased Fstl1 expression in heart (Fig. 4*A*). Quantitative Western blot analysis revealed an ∼2.5-fold increase in expression of Fstl1 protein in the whole heart of Fstl1-TG mice. Fstl1-TG mice also displayed a 5.7-fold increase in serum levels of Fstl1 protein (Fig. 4*A*). In skeletal muscle, Fstl1 levels were increased by approximately ninefold (Fig. S3*A*), but this increase did not lead to detectable changes in muscle or overall body weight (Fig. S3 *B* and *C*). Fstl1-TG mice showed no alterations in HW/BW or LW/BW ratios, septal or posterior ventricular wall thicknesses, ventricular chamber dimensions, or fractional shortening under baseline conditions (Fig. 4 *B–G*). Histological analysis also revealed no gross morphological alterations or detectable changes in myocyte size or fibrosis at baseline (Fig. 5 *A–C*).

Fstl1-TG mice and their WT C57BL/6 littermates were subjected to pressure overload caused by TAC. Fstl1-TG mice demonstrated a reduction in myocardial hypertrophy following TAC compared with age-matched WT littermates. Four weeks after TAC, the HW/BW ratio had increased to 24.5% in Fstl1-TG mice compared with 45.8% in WT mice (Fig. 4*B*). Further, the LW/BW ratio was reduced in Fstl1-TG mice compared with WT mice, indicative of diminished pulmonary congestion (Fig. 4*C*). The overexpression of Fstl1 attenuated the hypertrophic response and the decline in LV performance as assessed by echocardiography. In response to TAC, measured values for interventricular septum, posterior wall, and LV end diastolic dimensions were all diminished in Fstl1-TG mice compared with WT mice, whereas fractional shortening was improved (Fig. 4 *D–G*).

Cardiomyocyte cell size and interstitial fibrosis also were quantified on histological sections from WT and Fstl1-TG mice following TAC or sham surgery. Consistent with the diminished HW/BW ratio, Fstl1-TG mice showed less myocyte enlargement and diminished interstitial fibrosis than WT mice following TAC (Fig. 5 *A–C*). Moreover, Fstl1-TG mice displayed attenuated increases in BNP and ANF gene expression in response to TAC (Fig. 5 *D* and *E*). Under these conditions, Fstl1-TG mice displayed an increase in myocardial capillary density (Fig. S1).

To investigate the regulation of AMPK signaling in the Fstl1-TG model following pressure overload, the phosphorylation of the α2 subunit of AMPK in the heart was assessed by Western blot analysis. AMPK phosphorylation at Thr172 was increased in response to TAC in WT mice, as expected, but was significantly greater in Fstl1-TG mice (Fig. 5*F*). The cardiac expression of total AMPK protein did not differ in TG and WT mice either before or after TAC, and there were no detectable differences in AMPK phosphorylation in sham-operated hearts of Fstl1-TG and WT mice (Fig. 5*F*). Fstl1-TG mice displayed an increase in eNOS phosphorylation at Ser1179 under conditions of TAC, but there was no effect on SMAD2 phosphorylation (Fig. S2).

To test whether acute overexpression of Fstl1 could protect the heart from pressure overload, an adenoviral vector expressing

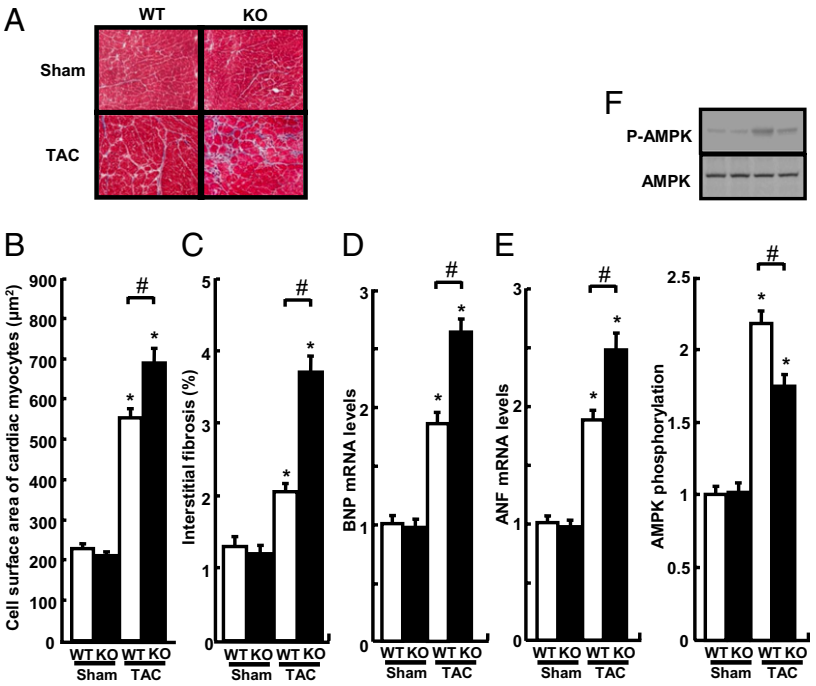

Fig. 3. Fstl1 deficiency in cardiac myocytes promotes TAC-induced myocyte hypertrophy and attenuates AMPK activation. (*A*) Representative histological sections from the left ventricle of WT and KO mice stained with Masson's trichrome. Heart samples were collected and processed 4 wk after TAC or sham surgery. (Magnification, 400x.) (*B* and *C*) Quantitative analysis of the CSA of cardiomyocytes (*B*) and intestinal fibrosis area (*C*) from each experimental group. Results are presented as mean ± SEM (n = 6–12 mice per group). (*D* and *E*) The results of qRT-PCR analysis of BNP (*D*) and ANF (*E*) expression. (*F*) Phosphorylation of AMPK (P-AMPK) at Thr172 in the hearts of WT and KO mice 1 wk after TAC or sham surgery. (*Upper*) Representative blots of phosphorylated and total AMPK. (*Lower*) Quantitative analysis of AMPK phosphorylation. Relative levels of AMPK phosphorylation were normalized to control values in sham-treated WT mice. n = 8 samples per group. $^{*}P < 0.05$ versus corresponding sham-treated mice; $^{\#}P < 0.05$ versus WT mice.

Fstl1 (Ad-Fstl1) or β-galactosidase (Ad-βgal) was delivered systemically to WT or Fstl1-KO mice 3 d before TAC surgery. At the time of surgery, an increase in circulating Fstl1 levels could be detected in Ad-Fstl1–treated mice by Western blot analysis of the serum (Fig. S4*A*). Adenovirus-mediated expression of Fstl1 attenuated the TAC-induced increase in the HW/BW ratio in both WT and KO mice at 4 wk (Fig. S4*B*). Acute Fstl1 delivery also increased ventricular performance in both mouse strains as indicated by a decrease in LV dimension and an increase in fractional shortening (Fig. S4 *C* and *D*). Adenovirus-mediated Fstl1 delivery had no effect on cardiac parameters in WT mice at baseline (Fig. S4*E*).

Fstl1 Attenuates Hypertrophy in Cultured Cardiomyocytes. To evaluate the antihypertrophic actions of Fstl1 at a mechanistic level, we investigated whether Fstl1 affects pathological hypertrophy in isolated neonatal rat ventricular cardiomyocytes (NRVMs). Before stimulation with 100 μmol/L phenylephrine (PE) or vehicle, NRVMs were infected with Ad-Fstl1 or with Ad-βgal as a control. Adenovirus-mediated *Fstl1* gene delivery significantly reduced the increase in cardiomyocyte cell surface area (CSA) induced by PE compared with Ad-βgal infection (Fig. 6*A*). Transduction with Ad-Fstl1 also attenuated the PE-induced increases in BNP and ANF gene expression (Fig. 6 *B* and *C*). To corroborate these findings, purified recombinant mouse Fstl1 protein, produced in SF-9 insect cells, was applied to NRVMs before PE treatment. Treatment with purified Fstl1 protein also led to a significant attenuation of PE-induced cardiac hypertrophy (Fig. 6*D*).

To examine the regulation of the AMPK signaling axis by Fstl1 in greater detail, the phosphorylation of the AMPK α2 subunit at Thr172 was assessed by Western blot analysis in NRVMs. Treatment with purified Fstl1 protein led to a time- and dose-dependent increase in AMPK phosphorylation. Acute treatment of NRVMs with Fstl1 led to a more than twofold increase in AMPK phosphorylation by 30 min (Fig. 7*A*). Accordingly, Fstl1 treatment led to an increase in the phosphorylation of acetyl-CoA carboxylase (ACC) on Ser79, a downstream target of AMPK. The level of Fstl1 protein required for half-maximal AMPK phosphorylation was 87 ng/mL (Fig. 7*B*). To examine the causal role of AMPK activation in the antihypertrophic action of Fstl1, NRVMs were transduced with an adenoviral vector expressing a dominant-negative AMPK construct (Ad-dnAMPK) or Ad-βgal before treatment with Fstl1. The growth-inhibitory actions of Fstl1 were nullified by treatment with the dominant-negative AMPK vector (Fig. 7*C*).

Discussion

The secreted glycoprotein Fstl1 is up-regulated in heart in response to various cardiac stresses. Here we describe two mouse models, one that ablates Fstl1 in cardiac myocytes and one that overexpresses Fstl1 in striated muscle; we used these models to examine the role of this factor in the control of heart growth. Neither Fstl1 ablation nor overexpression influenced heart size or function under baseline conditions. However, further analyses of these models revealed that Fstl1 functions as a negative regulator of cardiac growth under conditions of pressure overload-induced hypertrophy. Cardiac myocyte-selective *Fstl1* gene disruption led to exacerbated cardiac hypertrophy and greater LV systolic dysfunction at 4 wk post-TAC. Conversely, acute or chronic Fstl1 overexpression attenuated myocardial hypertrophy and LV systolic dysfunction after TAC injury. Fstl1 treatment also attenuated PE-induced hypertrophy in cultured cardiac myocytes. These data show that Fstl1 has an antihypertrophic activity and protects against cardiac remodeling in response to pathological hypertrophic stimuli. These data also provide mouse genetic evidence that support the classification of Fstl1 as a cardiokine, i.e., a factor secreted by heart that influences cardiovascular function (5).

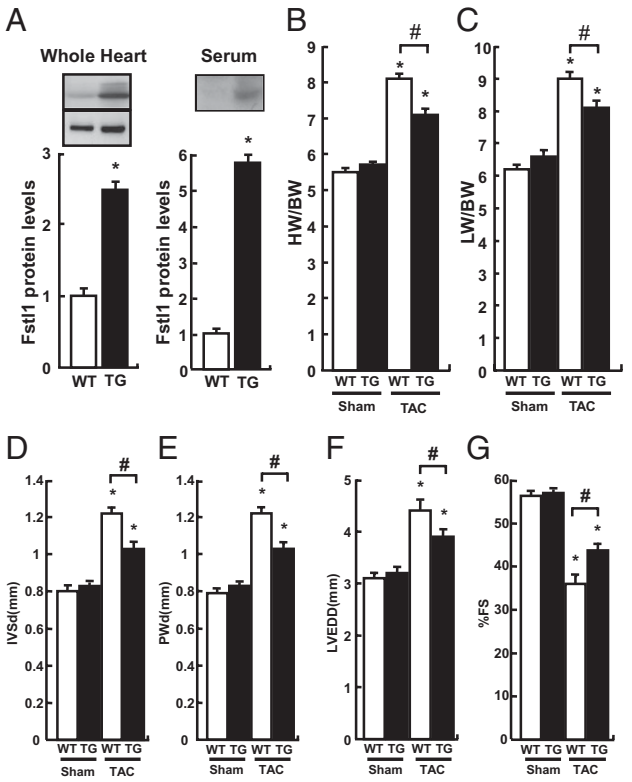

Fig. 4. Fstl1 overexpression protects against the development of cardiac hypertrophy and heart failure following pressure overload. (*A*) Western blot analysis was performed to evaluate Fstl1 protein expression in whole heart or serum in WT or striated muscle-specific Fstl1-TG mice. (*B* and *C*) HW/BW (*B*) and LW/BW (*C*) ratios in WT and Fstl1-TG mice 4 wk after TAC or sham surgery. (*D*–*G*) Echocardiographic measurements of IVSd (*D*), PWd (*E*), LVEDD (*F*), and %FS (*G*) for WT and TG mice 4 wk after TAC or sham surgery. For sham-treated mice, $n = 6$ WT and 6 TG mice. For TAC-treated mice, $n = 12$ WT mice and 13 TG mice. $^{*}P < 0.05$ versus corresponding sham-treated mice; $^{\#}P < 0.05$ versus corresponding WT mice.

Fstl1 is expressed by a number of different cell types under baseline conditions (26), but few studies have examined the cell types that are responsible for its up-regulation in response to injury. When whole mouse heart is processed for analysis, Fstl1 expression is induced following TAC as well as by injuries resulting from ischemia–reperfusion and permanent ligation of the left anterior descending (LAD) coronary artery (11). A previous study reported that the *Fstl1* transcript is expressed by multiple cell types, including vascular endothelial cells, smooth muscle cells, and cardiac myocytes, in explanted hearts from patients with end-stage heart failure (12). Thus, it is difficult to know the precise cell-type source(s) that are responsible for the induction of Fstl1 expression in heart following various cardiac injuries. When Cre recombinase is used to ablate Fstl1 specifically in α-myosin heavy-chain (αMHC)-expressing cells in the mouse, it is apparent that a substantial fraction of injury-induced Fstl1 expression is derived from cardiac myocytes following pressure-overload hypertrophy. The mouse strain used in this study effectively ablates Fslt1 in ventricular myocytes isolated from heart (>95%), but Fstl1 transcript and protein expression were reduced only 42% and 46%, respectively, in the Fstl1-KO hearts under baseline conditions. Thus, approximately half of Fstl1 expression is derived from the nonmyocyte compartment in uninjured hearts. On the other hand, TAC leads to a 9.5-fold increase in Fstl1 transcript and a 2.1-fold increase in protein expression, and this induction is largely nullified in the Fstl1-KO strain. Similarly, the increase in serum Fstl1 in response to TAC is reduced markedly in myocyte-specific Fstl1-KO mice. These data indicate that myocytes are the major source of Fstl1 induced by pressure overload in the heart. Consistent with this notion, considerable colocalization of Fstl1 and the myocyte marker protein α-actinin could be detected by confocal microscopy image analysis in WT but not in KO hearts, and this signal is induced markedly in myocytes following TAC. Interestingly, Fstl1 is expressed at very low levels in the developing myocardium (27, 28). Therefore, the injury-mediated induction of Fstl1 reported here probably does not represent a component of a reactivated fetal gene program but instead is likely to represent a feature of a general stress response.

The follistatin family of proteins generally is believed to function by binding to and modifying the function of members of the TGF-β family. For example, follistatin-like 3 (Fstl3) binds to activin A and can modulate the heart's response to ischemic stress (7) and pressure overload (29). Although Fstl1 may function as an extracellular regulator of TGF-β family proteins in some scenarios, such as during development (30), we currently do not favor this hypothesis to account for Fstl1's anti-hypertrophic actions in the pressure-overloaded heart. In this regard, Fstl1 shares a limited homology with follistatin and Fstl3, and it can function to activate intracellular signaling pathways rapidly in cardiovascular cells that are cultured in the absence of TGF-β family proteins (11, 31). As shown here, cardiac Smad2 signaling, a downstream target of canonical TGF-β family proteins in heart (29), is not altered in the Fstl1-KO or Fstl1-TG lines. Similarly, experiments in cultured myocytes have found no regulation of Smad2 by Fstl1 (32). Additionally, transgenic expression of Fstl1 from the striated muscle-specific creatine kinase M promoter had no effect on skeletal muscle mass or body weight, in marked contrast to other follistatin family members whose transgenic overexpression increased muscle mass (33). Therefore, in this experimental context, Fstl1 appears to function independently of TGF-β family proteins.

Here we show that Fstl1 promotes the rapid, activating phosphorylation of AMPK in hearts subjected to TAC and in cardiac myocytes cultured in low-mitogen medium. The dose of recombinant Fstl1 protein required for half-maximal AMPK phosphorylation was 87 ng/mL, a level consistent with levels of circulating Fstl1 reported in healthy individuals (median = 7.18 ng/mL; range = 1.06–18.49 ng/mL) and in individuals with acute coronary syndrome (median = 13.50 ng/mL; range = 8.82–30.46 ng/mL) (22). Fstl1 can exert its actions via the candidate receptor Disco-interacting protein 2 homolog A (DIP2A) (15, 16); however, preliminary analyses of whether DIP2A mediates Fstl1 actions on AMPK signaling in myocytes have been inconclusive.

Consistent with observations of AMPK activation, an increase in myocardial eNOS phosphorylation at Ser1179 was observed in Fstl1-TG mice following TAC, whereas this phosphorylation was reduced in Fstl1-KO mice. AMPK is capable of directly phosphorylating eNOS on this residue, leading to the production of NO (34). It is widely recognized that NO inhibits maladaptive cardiac hypertrophy (35), and this signaling action could contribute mechanistically to the cardioprotective actions of Fstl1. In addition, NO is widely recognized as being critical in angiogenic responses (36), and hearts from Fstl1-KO mice displayed a reduction in capillary density following TAC, whereas hearts from Fstl1-TG mice displayed an increase in capillary density following TAC. These effects on myocardial capillarization are consistent with the previously described angiogenic functions of Fstl1 (31) and AMPK signaling (32, 34, 37). Because a diminished angiogenic response to TAC can facilitate the transition from cardiac hypertrophy to heart failure (9, 32, 38), the proangiogenic activity of Fstl1 is likely to contribute to its cardioprotective function in this model.

AMPK activity is enhanced in rodent hearts after pressure-overload injury (8, 39), and gene ablation studies indicate that cardiac AMPK α2-subunit protects against the development of ventricular hypertrophy and remodeling (25). Consistent with these

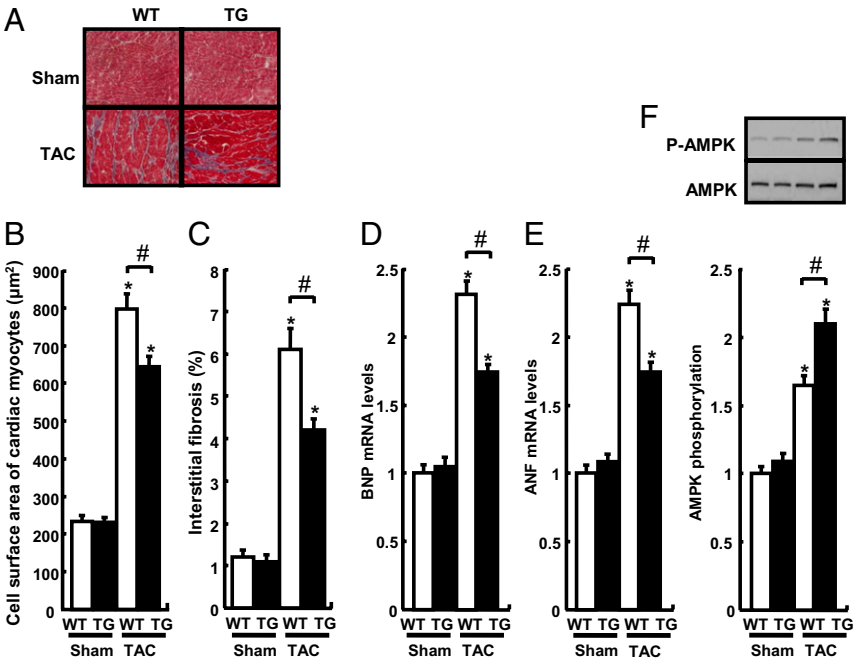

Fig. 5. Gain of Fstl1 function attenuates myocyte hypertrophy and fibrosis and promotes AMPK activation in response to TAC. (*A*) Representative histological left ventricle sections from WT and TG mice treated with Masson trichrome stain. Heart samples were collected 4 wk after TAC or sham surgery. (Magnification, 400×.) (*B* and *C*) Quantitative analysis of the cardiomyocyte CSA (*B*) and intestinal fibrosis (*C*) from each experimental group. Results are presented as mean ± SEM (n = 6–12 mice per group). (*D* and *E*) The results of qRT-PCR analysis of BNP (*D*) and ANF (*E*) expression. (*F*) P-AMPK in the hearts of WT and TG mice 1 wk after TAC or sham surgery. (*Upper*) Representative blots of phosphorylated and total AMPK. (*Lower*) Quantitative analysis of AMPK phosphorylation. Relative phosphorylated levels of AMPK were normalized to control values in sham-treated WT mice (n = 8 hearts per group). *$P < 0.05$ versus corresponding sham-treated mice; $^{\#}P < 0.05$ versus WT mice.

in vivo observations, activation of AMPK by pharmacological reagents, such as metformin or resveratrol, can reduce agonist-stimulated protein synthesis and cellular growth in cultured cardiac myocytes (40, 41). Peptide regulators of cardiac AMPK include the adipokine adiponectin (8) and the inflammation-regulatory protein macrophage migration inhibitory factor (MIF) (42). Although both adiponectin and MIF have a cardioprotective function, MIF is more similar to Fstl1 in that it is induced by cardiac injury and functions as an autocrine/paracrine regulator of AMPK.

A number of studies have reported that Fstl1 has complex roles in the control of inflammatory cells. It has been shown that Fstl1 expression can be induced by innate immune signals and promote proinflammatory cytokine expression leading to T-cell activation in a model of arthritis (18, 20). Consistent with a proinflammatory role, Fstl1 is elevated in patients with various systemic autoimmune diseases or acute coronary syndrome (22, 43, 44). On the other hand, it also has been reported that Fstl1 overexpression ameliorates experimental arthritis and prolongs heart allograft survival by inhibiting proinflammatory cytokine expression (19, 45). Excluding cardiac transplantation, nothing is known about the role of Fstl1 in controlling inflammation in the heart. Although the pressure-overload model used here elicits a relatively modest immune response, models of myocardial ischemia/reperfusion and permanent LAD ligation cause cellular necrosis and provide strong inflammatory stimulation (46). Thus, it will be of interest for future studies to investigate the cell type-specific roles of Fstl1 in modulating cardiac inflammation in response to ischemic injuries.

In summary, we show that Fstl1 functions as an injury-induced, antihypertrophic "cardiokine" that activates AMPK signaling. Our work with cardiac myocyte-specific Fstl1-KO mice shows that the expression of Fstl1 following pressure overload can be attributed largely to its induced expression by myocytes within the heart and that it acts in an autocrine/paracrine manner to modulate hypertrophy. However, as also is shown here, Fstl1 is expressed in the nonmyocyte compartment within the heart, and these other cell types may have a more dominant role in expressing this factor in other types of cardiac injury. Unless future studies of Fstl1 action in the heart using a loss-of-function model take this issue into account, the role of Fstl1 in cardiac repair could be underestimated.

Materials and Methods

Materials. Antibodies against phospho-AMPK (Thr172), pan-α-AMPK, phospho-acetyl-CoA carboxylase (phospho-ACC) (Ser79), ACC, and GAPDH were

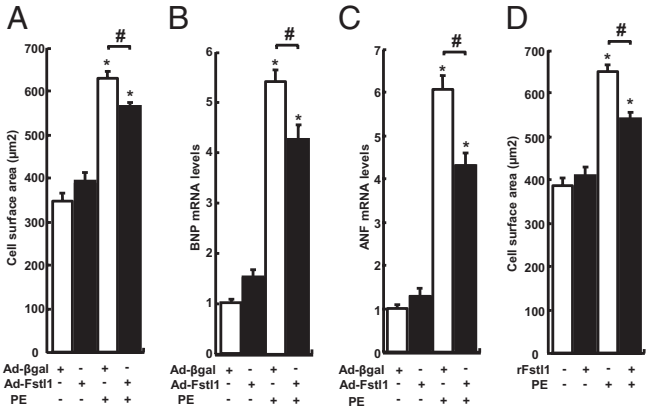

Fig. 6. Fstl1 attenuates the hypertrophic actions to PE treatment in cultured cardiac myocytes. (*A*) Quantitative analysis of PE-induced hypertrophy following transduction with adenoviral vector Ad-Fstl1 or Ad-βgal (control). Cultures of NRVMs were transduced at an MOI of 50 for 8 h. After 36 h of further incubation in fresh medium, cells were treated with PE for 24 h. (*B* and *C*) qRT-PCR analysis of BNP (*B*) and ANF (*C*) expression in cells transduced with Ad-Fstl1 or Ad-βgal in the presence or absence of PE (100 μmol/L) for 24 h. (*D*) Quantitative analysis of myocyte CSA after treatment with rFstl1 and PE. *$P <$ 0.05 versus corresponding control; $^{\#}P < 0.05$ versus control treatment.

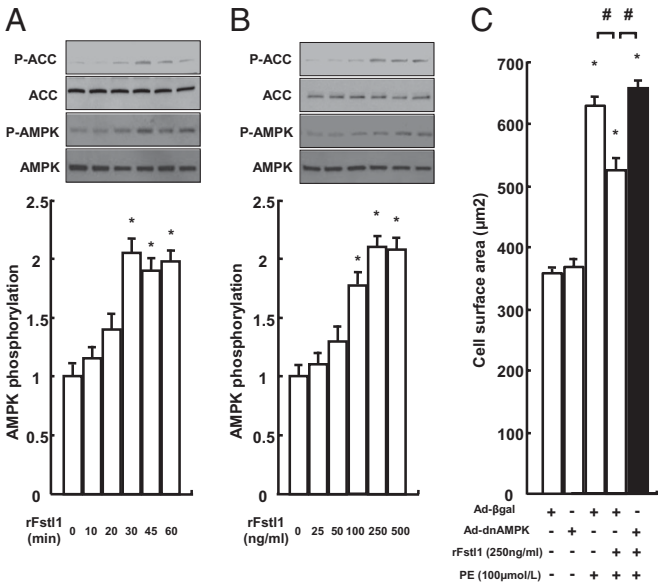

Fig. 7. Inhibition of PE-stimulated myocyte hypertrophy by Fstl1 is mediated by AMPK signaling. Time-dependent (*A*) and dose-dependent (*B*) changes in the phosphorylation of AMPK after rFstl1 treatment in NRVMs. (*A* and *B*, *Upper*) Representative blots of phosphorylated and total ACC and AMPK are shown. (*Lower*) Quantitative analysis of AMPK phosphorylation. (*C*) Quantitative analysis of CSA after infection with Ad-dnAMPK or Ad-βgal (control). After vector transduction for 8 h, cells were washed and incubated for 36 h before treatment with PE (100 μmol/L) in the presence or absence of rFstl1 (250 ng/mL). $^{*}P < 0.05$ versus corresponding control; $^{\#}P < 0.05$ versus Fstl1 treatment.

purchased from Cell Signaling Technology. Fstl1 antibody was obtained from R&D Systems. DMEM was purchased from Invitrogen.

Creation of Mouse Lines. To generate animals with targeted ablation of Fstl1 in cardiac myocytes, mice with loxP sites flanking the first protein-coding exon of the *Fstl1* gene (Fstl1$^{flox/flox}$) (47) were crossed with transgenic mice expressing cre recombinase under the control of the αMHC promoter (Jackson Laboratory) (48). αMHC-Cre$^{+/-}$ × Fstl1$^{flox/flox}$ mice were used as homozygous cardiac-specific Fstl1 gene-deficient mice, and αMHC-Cre$^{+/-}$ × Fstl1$^{+/+}$ mice were used as control mice. These mice are all were maintained in the FVB genetic background. Primer pairs used for genotyping PCR were Fstl1 forward: GCCAGAATCCCACTCCATCG and Fstl1 reverse: TCGGAGCCTGGTGATAAGCG. The Fstl1 floxed allele is detected as a 650-bp fragment, whereas the *Fstl1* WT allele gives a 411-bp fragment. The αMHC-Cre transgene was detected by using the primer pair 5′-ATGACAGACAGATCCCTCCTATCTCC-3′ and 5′-CTCATCACTCGTTGCATCATCGAC-3′ that amplifies a 300-bp fragment.

Fstl1-TG mice were generated by subcloning the mouse full-length Fstl1 cDNA, which encodes the full-length, 306-amino acid protein including the native signal sequence, into the EcoRV site of pBluescript vector with the 4.8-kb murine muscle creatine kinase (MCK) promoter (49). The MCK promoter is expressed in both cardiac and skeletal muscle, as is Fstl1 (11, 31). Thus, the MCK promoter was used to create the transgenic line because it approximates the expression pattern of endogenous Fstl1. The DNA fragment was excised and used for pronuclear injection. Positive founders were identified by PCR and bred to C57BL/6 mice to generate stable transgenic lines. Although the Fstl1-deficient line had an FVB background, the transgenic lines were in the C57BL/6 background. These differences in strain can influence the response to pressure-overload hypertrophy (10).

TAC Protocol. All procedures on mice were approved by the Institutional Animal Care and Use Committee of Boston University. Mice (8 wk old) were anesthetized with sodium pentobarbital (50 mg/kg i.p.). The chest was opened, and the thoracic aorta was exposed following dissection through the intercostal muscles. A 7–0 silk suture was placed around the transverse aorta and tied around a 26-gauge blunt needle, which subsequently was removed (8). Sham-operated mice underwent a similar surgical procedure without the constriction of the aorta. At the indicated time points, animals were anesthetized and then killed. The hearts and the lungs were removed and weighed.

Echocardiography. After 28 d, surviving mice were subjected to transthoracic echocardiography to determine cardiac function and structure. To measure LV systolic function and chamber dimensions, echocardiography was performed with an Acuson Sequoia C-256 machine using a 15-MHz probe. Diastolic intraventricular septum (IVSd), diastolic posterior wall thickness (PWd), LV end diastolic diameter (LVEDD), and percent LV fractional shortening (% FS) were assessed from M-mode images.

Histology. Mice were killed and LV tissue was obtained 4 wk after the TAC procedure. Heart samples were embedded in Optimal Cutting Temperature compound (Miles Laboratories) and frozen in liquid nitrogen. Tissue slices (7 um in thickness) were prepared. To determine the myocyte CSA and levels of interstitial fibrosis, sections were stained with H+E and Masson's trichrome, respectively. CSA and fibrosis were quantified as described previously (38). To quantify the percent fibrosis, microscopic images stained with Masson trichrome were digitized with Viewfinder Light Image (Mitani). The blue pixel content of digitized images was measured relative to total tissue area using the image analyzer Win ROOF (Mitani). For immunofluorescence, myocardial tissues from WT or KO mice were fixed by 4% paraformaldehyde and incubated with Fstl1 antibody (R&D Systems), followed by incubation with biotin-conjugated secondary antibody and HRP-avidin. Tissues were blocked with BSA and the M.O.M. kit (Vector Laboratories) and incubated with Fstl1 antibody and α-actinin antibody (EA53; Sigma), followed by incubation with Alexa Fluor 488 for detection of Fstl1 and Alexa Fluor 594 for detection of α-actinin–conjugated secondary antibody. Images were recorded using Zeiss LSM 710-Live DuoScan confocal microscopy.

Primary NRVM Culture and Isolation of Adult Mouse Ventricular Cardiac Myocytes. Primary cultures of NRVMs were prepared as described previously (50). NRVMs were incubated in DMEM supplemented with 7% FCS for 18 h after preparation and subsequently were transfected with the adenoviral vectors Ad-Fstl1 or Ad-βgal at a multiplicity of infection (MOI) of 50 for 8 h in DMEM (11). The medium then was replaced with fresh DMEM without adenovirus. Thirty-six hours after infection, NRVMs were incubated with PE (100 μmol/L) for 24 h. NRVMs were incubated with recombinant mouse Fstl1 protein (rFstl1) for the indicated length of time. Fstl1 protein tagged with FLAG in the N terminus was prepared in SF9 cells with minor modifications of the procedure described previously (15). In other experiments, NRVMs were treated with adenoviral vector expressing Ad-dnAMPK or Ad-βgal at an MOI of 50 for 8 h (8). After infection, NRVMs were incubated with rFstl1 for the indicated length of time. In the other experiment, adult mouse ventricular cardiac myocytes were isolated according to procedures described previously (7) following Alliance for Cell Signaling protocols.

Western Blot Analysis. Tissue samples obtained on postoperative day 7 were homogenized in lysis buffer (Cell Signaling Technology) with a protease inhibitor mixture (Sigma) and phosphatase mixture inhibitor (Calbiochem). Protein content was determined by the Bradford method. Equal amounts of protein (40 μg) were separated in denaturing SDS 8–12% polyacrylamide gels and transferred to nitrocellulose membranes. Membranes were immunoblotted with the primary antibodies at a 1:1,000–5,000 dilution followed by incubation with the secondary antibody conjugated with HRP at a 1:1,000–10,000 dilution. Proteins were visualized using ECL Western Blotting Detection kit (Amersham Pharmacia Biotech).

RNA Isolation and Quantitative Real-Time PCR. Total RNA was prepared from mouse heart by using a RNA isolation kit for fibrous tissue, and total RNA from cultured cells was prepared with a RNA isolation kit (Qiagen). cDNA was synthesized from 500 ng of total RNA using the SuperScript RT-PCR System (Invitrogen). qRT-PCR was carried out on an iCycler (Bio-Rad) using SYBR green (Applied Biosystems). The following primer sequences were used: mouse, GAPDH forward: 5′-TCACCACCATGGAGAAGGC-3′, reverse: 5′-GCTAAGCAGTTGGTGGTGCA-3′; Fstl1 forward: 5′-AACAGCCATCAACATCACCACTTAT-3′, reverse: 5′-TTTCCAGTCAGCGTTCTCATCA-3′; rat, GAPDH forward: 5′-TCAAGAAGGTGGTGAAGCAG-3′, reverse: 5′-AGGTGGAAGAATGGGAGTTG-3′; Fstl1 forward: 5′-CTGAAATTCGTGGAGGAGAA-3′, reverse: 5′-GTTTCCAGTCAGCGTTCTCA-3′. The expression levels of examined transcripts were compared with that of GAPDH and normalized to the mean value of controls.

Statistical Analysis. Data are presented as mean ± SEM. Group differences were analyzed by two-tailed Student's *t* test or ANOVA. To compare multiple groups, a Mann–Whitney *U* test with Bonferroni correction was used. A value of $P < 0.05$ was considered statistically significant.

ACKNOWLEDGMENTS. This study was funded by National Institutes of Health Grants HL102874, AG34972, AG15052, and HL68758 (to K.W.), Grant-in-Aid for Young Scientists B23790844 (to M.S.), Netherlands Heart Foundation Grant 1996M002, and European Community's Sixth Framework Program contract ("HeartRepair") Grant LSHM-CT-2005-018630 (to M.J.B.v.d.H. and B.v.W.).

1. Levy D, Garrison RJ, Savage DD, Kannel WB, Castelli WP (1990) Prognostic implications of echocardiographically determined left ventricular mass in the Framingham Heart Study. *N Engl J Med* 322:1561–1566.
2. Molkentin JD, Dorn GW, 2nd (2001) Cytoplasmic signaling pathways that regulate cardiac hypertrophy. *Annu Rev Physiol* 63:391–426.
3. Frey N, Katus HA, Olson EN, Hill JA (2004) Hypertrophy of the heart: A new therapeutic target? *Circulation* 109:1580–1589.
4. Frost RJ, Engelhardt S (2007) A secretion trap screen in yeast identifies protease inhibitor 16 as a novel antihypertrophic protein secreted from the heart. *Circulation* 116:1768–1775.
5. Doroudgar S, Glembotski CC (2011) The cardiokine story unfolds: Ischemic stress-induced protein secretion in the heart. *Trends Mol Med* 17:207–214.
6. Heineke J, et al. (2010) Genetic deletion of myostatin from the heart prevents skeletal muscle atrophy in heart failure. *Circulation* 121:419–425.
7. Oshima Y, et al. (2009) Activin A and follistatin-like 3 determine the susceptibility of heart to ischemic injury. *Circulation* 120:1606–1615.
8. Shibata R, et al. (2004) Adiponectin-mediated modulation of hypertrophic signals in the heart. *Nat Med* 10:1384–1389.
9. Shiojima I, et al. (2005) Disruption of coordinated cardiac hypertrophy and angiogenesis contributes to the transition to heart failure. *J Clin Invest* 115: 2108–2118.
10. Xu J, et al. (2006) GDF15/MIC-1 functions as a protective and antihypertrophic factor released from the myocardium in association with SMAD protein activation. *Circ Res* 98:342–350.
11. Oshima Y, et al. (2008) Follistatin-like 1 is an Akt-regulated cardioprotective factor that is secreted by the heart. *Circulation* 117:3099–3108.
12. Lara-Pezzi E, et al. (2008) Expression of follistatin-related genes is altered in heart failure. *Endocrinology* 149:5822–5827.
13. Mashimo J, Maniwa R, Sugino H, Nose K (1997) Decrease in the expression of a novel TGF beta1-inducible and ras-recision gene, TSC-36, in human cancer cells. *Cancer Lett* 113:213–219.
14. Shibanuma M, Mashimo J, Mita A, Kuroki T, Nose K (1993) Cloning from a mouse osteoblastic cell line of a set of transforming-growth-factor-beta 1-regulated genes, one of which seems to encode a follistatin-related polypeptide. *Eur J Biochem* 217: 13–19.
15. Ouchi N, et al. (2010) DIP2A functions as a FSTL1 receptor. *J Biol Chem* 285:7127–7134.
16. Tanaka M, et al. (2010) DIP2 disco-interacting protein 2 homolog A (Drosophila) is a candidate receptor for follistatin-related protein/follistatin-like 1—analysis of their binding with TGF-β superfamily proteins. *FEBS J* 277:4278–4289.
17. Chan QK, et al. (2009) Tumor suppressor effect of follistatin-like 1 in ovarian and endometrial carcinogenesis: A differential expression and functional analysis. *Carcinogenesis* 30:114–121.
18. Clutter SD, Wilson DC, Marinov AD, Hirsch R (2009) Follistatin-like protein 1 promotes arthritis by up-regulating IFN-gamma. *J Immunol* 182:234–239.
19. Kawabata D, et al. (2004) Ameliorative effects of follistatin-related protein/TSC-36/FSTL1 on joint inflammation in a mouse model of arthritis. *Arthritis Rheum* 50: 660–668.
20. Miyamae T, et al. (2006) Follistatin-like protein-1 is a novel proinflammatory molecule. *J Immunol* 177:4758–4762.
21. Schiekofer S, et al. (2006) Microarray analysis of Akt1 activation in transgenic mouse hearts reveals transcript expression profiles associated with compensatory hypertrophy and failure. *Physiol Genomics* 27:156–170.
22. Widera C, et al. (2009) Circulating concentrations of follistatin-like 1 in healthy individuals and patients with acute coronary syndrome as assessed by an immunoluminometric sandwich assay. *Clin Chem* 55:1794–1800.
23. El-Armouche A, et al. (2011) Follistatin-like 1 in chronic systolic heart failure: A marker of left ventricular remodeling. *Circ Heart Fail* 4(5):621–627.
24. Ikeda Y, et al. (2009) Cardiac-specific deletion of LKB1 leads to hypertrophy and dysfunction. *J Biol Chem* 284:35839–35849.
25. Zhang P, et al. (2008) AMP activated protein kinase-alpha2 deficiency exacerbates pressure-overload-induced left ventricular hypertrophy and dysfunction in mice. *Hypertension* 52:918–924.
26. Arai KY, Tsuchida K, Uehara K, Taya K, Sugino H (2003) Characterization of rat follistatin-related gene: Effects of estrous cycle stage and pregnancy on its messenger RNA expression in rat reproductive tissues. *Biol Reprod* 68:199–206.
27. van den Berg G, Somi S, Buffing AA, Moorman AF, van den Hoff MJ (2007) Patterns of expression of the Follistatin and Follistatin-like1 genes during chicken heart development: A potential role in valvulogenesis and late heart muscle cell formation. *Anat Rec (Hoboken)* 290:783–787.
28. Adams D, Larman B, Oxburgh L (2007) Developmental expression of mouse Follistatin-like 1 (Fstl1): Dynamic regulation during organogenesis of the kidney and lung. *Gene Expr Patterns* 7:491–500.
29. Shimano M, et al. (2011) Cardiac myocyte-specific ablation of follistatin-like 3 attenuates stress-induced myocardial hypertrophy. *J Biol Chem* 286:9840–9848.
30. Geng Y, et al. (2011) Follistatin-like 1 (Fstl1) is a bone morphogenetic protein (BMP) 4 signaling antagonist in controlling mouse lung development. *Proc Natl Acad Sci USA* 108:7058–7063.
31. Ouchi N, et al. (2008) Follistatin-like 1, a secreted muscle protein, promotes endothelial cell function and revascularization in ischemic tissue through a nitric-oxide synthase-dependent mechanism. *J Biol Chem* 283:32802–32811.
32. Shimano M, et al. (2010) Adiponectin deficiency exacerbates cardiac dysfunction following pressure overload through disruption of an AMPK-dependent angiogenic response. *J Mol Cell Cardiol* 49:210–220.
33. Lee SJ (2007) Quadrupling muscle mass in mice by targeting TGF-beta signaling pathways. *PLoS ONE* 2:e789.
34. Ouchi N, et al. (2004) Adiponectin stimulates angiogenesis by promoting cross-talk between AMP-activated protein kinase and Akt signaling in endothelial cells. *J Biol Chem* 279:1304–1309.
35. Kempf T, Wollert KC (2004) Nitric oxide and the enigma of cardiac hypertrophy. *Bioessays* 26:608–615.
36. Murohara T, et al. (1998) Nitric oxide synthase modulates angiogenesis in response to tissue ischemia. *J Clin Invest* 101:2567–2578.
37. Ouchi N, Shibata R, Walsh K (2005) AMP-activated protein kinase signaling stimulates VEGF expression and angiogenesis in skeletal muscle. *Circ Res* 96:838–846.
38. Izumiya Y, et al. (2006) Vascular endothelial growth factor blockade promotes the transition from compensatory cardiac hypertrophy to failure in response to pressure overload. *Hypertension* 47:887–893.
39. Tian R, Musi N, D'Agostino J, Hirshman MF, Goodyear LJ (2001) Increased adenosine monophosphate-activated protein kinase activity in rat hearts with pressure-overload hypertrophy. *Circulation* 104:1664–1669.
40. Chan AY, Soltys CL, Young ME, Proud CG, Dyck JR (2004) Activation of AMP-activated protein kinase inhibits protein synthesis associated with hypertrophy in the cardiac myocyte. *J Biol Chem* 279:32771–32779.
41. Chan AY, et al. (2008) Resveratrol inhibits cardiac hypertrophy via AMP-activated protein kinase and Akt. *J Biol Chem* 283:24194–24201.
42. Miller EJ, et al. (2008) Macrophage migration inhibitory factor stimulates AMP-activated protein kinase in the ischaemic heart. *Nature* 451:578–582.
43. Li D, et al. (2011) Follistatin-like protein 1 is elevated in systemic autoimmune diseases and correlated with disease activity in patients with rheumatoid arthritis. *Arthritis Res Ther* 13(1):R17.
44. Wilson DC, et al. (2010) Follistatin-like protein 1 is a mesenchyme-derived inflammatory protein and may represent a biomarker for systemic-onset juvenile rheumatoid arthritis. *Arthritis Rheum* 62:2510–2516.
45. Le Luduec JB, et al. (2008) An immunomodulatory role for follistatin-like 1 in heart allograft transplantation. *Am J Transplant* 8:2297–2306.
46. Frangogiannis NG (2004) Chemokines in the ischemic myocardium: From inflammation to fibrosis. *Inflamm Res* 53:585–595.
47. Silva M, et al. (2011) The BMP antagonist follistatin-like 1 is required for skeletal and lung organogenesis. *PLoS One* 6(8):e22616.
48. Agah R, et al. (1997) Gene recombination in postmitotic cells. Targeted expression of Cre recombinase provokes cardiac-restricted, site-specific rearrangement in adult ventricular muscle in vivo. *J Clin Invest* 100:169–179.
49. Sternberg EA, et al. (1988) Identification of upstream and intragenic regulatory elements that confer cell-type-restricted and differentiation-specific expression on the muscle creatine kinase gene. *Mol Cell Biol* 8:2896–2909.
50. Pimentel DR, et al. (2001) Reactive oxygen species mediate amplitude-dependent hypertrophic and apoptotic responses to mechanical stretch in cardiac myocytes. *Circ Res* 89:453–460.